Appendix A

The Delta Smelt individual-based model in R

Introduction

The delta smelt individual-based life cycle model in R (IBMR) simulates four processes of the San Francisco Estuary's delta smelt population: reproduction, movement, growth, and mortality. The model provides a mechanistic description of the life cycle, synthesizing the most recent life history information. Environmental variation representing dimensions of delta smelt habitat were temperature, turbidity, Old and Middle River flow, and prey density.

The IBMR is a modification of the IBM in Fortran (IBM), developed by Rose et al. (2013a). By design, many features of IBMR are identical to the original IBM, but IBMR was developed to be more accessible by using a more commonly used statistical program with open-source code that can be accessed and run by any R-user (R 2022). IBMR has been updated to include current models of delta smelt population dynamics, including fecundity, mortality, and the sensitivity of growth to environmental conditions. IBMR was calibrated to abundances and growth rates estimated for the wild delta smelt population from 1995 to 2014. The model is suitable for assessing the population growth potential of delta smelt, given observed or predicted changes to abiotic and biotic conditions in the SFE.

Updates. Several variations of a delta smelt individual-based life cycle model have been developed since Rose et al. (2013a) published their original IBM. A summary of the version history of these model variations is included in Table A1. In IBMR all data were updated for years 1995 through 2014, and all IBMR processes occurred on a monthly time step, rather than the hourly (movement) to daily (vital rate) time steps of the IBM. The coarser temporal scale of IBMR facilitated faster processing. The spawning model was modified to include up to three spawning opportunities per individual, with the third spawning event in April conditional on temperature and survival (LaCava et al. 2015; Kurobe et al. 2016). IBMR also included a turbidity effect on foraging rates documented by Hasenbein et al. (2016) for delta smelt and by Pangle et al. (2012) for other fish species occupying a similar ecological niche to delta smelt. The bioenergetics model was further updated to include additional prey types developed for an update to the Fortran IBM (Slater and Baxter 2014; Smith and Nobriga 2023), and the model of individual fecundity was updated based on the most recent published information (Damon et al. 2016). Finally, a recently developed statistical life cycle model for delta smelt (Smith et al. 2021) was used to update IBMR with estimates of the proportion of the population lost to entrainment during water export from the South Delta. In IBMR version 2, the consumption component of the bioenergetics model was updated to include recently estimated parameters that refit the relationship between temperature and consumption of prey (Smith and Nobriga 2023).

Data

Five physical and biological variables, representing observed Delta conditions during 1995-2014, drive simulated population dynamics: prey density, Old and Middle River flow, delta smelt distribution, water temperature, and Secchi depth. All data used to summarize IBMR variables may be found online (https://github.com/CSAMP). All variables except Old and Middle River flow had dimensions year *y*, month *m*, and spatial strata *s* (Table A2). Old and Middle River flow was a *y* x *m* matrix, and prey densities included a fourth dimension *p* indexing prey type.

Prey density. Prey density estimates PD_{ymsp} for 12 zooplankton prey types *p* and years 1989-2015 were developed by Wim Kimmerer (Table A3; personal communication). Mean log prey carbon densities (mgC m^{-3}), estimated from positive catches, and proportion zero catch were summarized from the Interagency Ecological Program's zooplankton survey and the CA Department of Fish and Wildlife (CDFW) 20-mm Survey. When a small sequence of samples were missing for a taxa-region combination, linear interpolation was used to predict the missing values, and when many sequential samples were missing, the missing data were predicted from general linear models fit using data from neighboring regions as predictors.

Old and Middle River flow. OMR_{ym} was the monthly average of the daily sum of tidally filtered flows (ft^3 s^{-1}) from two adjacent channels of the San Joaquin River basin, Old and Middle Rivers (Fig. A1). *OMR* data were available from US Geological Survey (USGS) streamflow databases (https://waterdata.usgs.gov). Much of the daily streamflow gauge data was missing. If data for one river was missing, daily *OMR* was predicted from a linear model of the flow in the remaining river, and if data for both rivers was missing, linear interpolation was used to estimate the missing values.

Fish distribution. Observed delta smelt distributions DS_{yms} (proportion in each stratum) were developed from 20-mm, Midwater Trawl, and Spring Kodiak Surveys. Townet Survey data were not used, because tow volume data were unavailable before 2003, use of Townet data would only leverage one additional month of distribution information (August), and in most year-months with a concurrent 20-mm Survey sample, delta smelt were observed in fewer spatial strata in the Townet Survey (in 7 of 13 years). Fish survey data were made available online by CDFW (ftp://ftp.dfg.ca.gov/). Monthly observed catch densities (catch/volume sampled) were assigned to the 12 spatial strata, and month-strata mean observed densities were expanded to population abundance by multiplying by strata volumes. Strata volumes were estimated by Derek Hilts (USFWS; Bay-Delta Office) using DSM2. Estimated population abundances in each spatial stratum were then converted to proportions of the total abundance, which were interpreted as observed occupancy probabilities.

Surveys were not completed in all year-months, and in some months, no fish were observed (mostly February, March, and August). Distributions from the prior month were assumed when observations were missing. The fish distribution data was characterized by an increasing level of zero-inflation, resulting in zero observed occupancy of many spatial strata towards the end of the time series. 2014 was selected as the terminal cohort of observed spatial distributions (last observed in April 2015) in order to mitigate this issue.

Delta smelt densities in the South Delta spatial stratum were particularly difficult to characterize, with many instances in which entrained delta smelt were observed at the pumping facilities, but

not in the South Delta fish surveys. The Delta Smelt Life Cycle Model (Smith et al. 2021) included estimates of the fraction of the population that entered the South Delta and were eliminated from the population (entrained). These estimates of proportional entrainment loss were developed by integrating multiple data sources, including salvage or observations of delta smelt at the pumping facilities. Life Cycle Model estimates of proportional entrainment were interpreted as the fraction of the population in the South Delta, and adopted as IBMR estimates of the South Delta distribution of delta smelt.

An alternative treatment of the South Delta distributions used the fish surveys to estimate proportion in the South Delta, like other strata; however, delta smelt densities in the South Delta stratum were depleted by entrainment, resulting in a negative bias and underestimation of the proportion of the population in this region of the Delta. Further, on many occasions, no fish were observed in the South Delta surveys, but one or more fish were salvaged, indicating that South Delta survey data were more zero-inflated than salvage data.

The conceptual model for the entrainment process is that under certain conditions, a fraction of the population is induced to occupy a portion of the Lower San Joaquin River, where they become vulnerable to advective flows (*OMR*) into the South Delta. Over a period of 1-2 weeks, the group of fish that moved into the South Delta becomes depleted by water exports until no or few fish remain. The model of delta smelt distributions did not account for the conditions leading fish to occupy the South Delta; it only accounted for the fraction of fish that were originally observed there.

Temperature. Water temperature data $Temp_{\mathrm{yms}}$ (Celsius) for years 1990-2010 were summarized from DSM2 hydrodynamic simulations by Derek Hilts (Fig. A1). The terminal year of the DSM2 *Temp* dataset, 2010, limited the number of years available for the IBMR by at least 4 years. A second set of water temperature data was therefore summarized from all available online data collected by the CDFW and FWS during Delta fish monitoring programs (ftp://ftp.dfg.ca.gov/; https://www.fws.gov/lodi/). The second water temperature dataset spanned years 1959-2020, but prior to 2011, data for some year-month-strata combinations were missing or sparse, with only a single sample.

The water temperatures that would have been simulated by DSM2 for missing years, 2011-2014, were predicted using a general linear model of DSM2 monthly means $Temp_{\mathrm{yms}}$ as a function of season, spatial strata, and monthly mean temperatures measured by fish monitoring programs $\widehat{Temp}_{\mathrm{yms}}$. The best model of $Temp_{\mathrm{yms}}$ was identified using backwards selection, starting with a full model, having an effect for each stratum and season, and eliminating non-significant spatial effects (acceptance level < 0.05), one coefficient at a time, before eliminating non-significant seasonal effects. The model was fit to data from years 1990-2010, and used to predict $Temp_{\mathrm{yms}}$ from measured $\widehat{Temp}_{\mathrm{yms}}$ for years 2011-2014. See Appendix B for details of the model to predict $Temp_{\mathrm{yms}}$.

Secchi depth. Secchi depth data $Secchi_{\mathrm{yms}}$ (cm) were used as an index of turbidity. Like $\widehat{Temp}_{\mathrm{yms}}$, Secchi depths for years 1959-2020 were summarized from all CDFW and FWS databases available

online (Fig. A1). Means for each year-month-stratum combination were summarized, but data were not available for all strata in all year-months. Missing data were estimated from general linear models of the remaining Secchi data in other spatial strata. The best general linear model for each stratum was selected using backwards selection, beginning with the full model, having a separate coefficient for each spatial stratum, and eliminating non-significant coefficients, one at a time.

Model

The IBMR (Fig. A2) includes cohorts spawned from 1995 to 2014. A cohort year begins at the beginning of simulated spawning in February and ends the following January. Reproduction, movement among 12 spatial strata, growth, and mortality of a closed population are modeled (Fig. A3). The simulated population in one year depends on the characteristics of the simulated population in the previous year; therefore, it is important to establish stable length and spatial distributions before simulating the 1995-2014 time series. IBMR establishes stable length and spatial distributions by looping through a representative sequence of years before simulating the 1995-2014 time series. The first (four) loops are discarded as a burn-in. This results in median fork lengths of 74 mm in the initial month of the simulation, February 1995.

Starting conditions. After the super-individual approach of the IBM, a super-adult approach was developed for IBMR. At the end of each simulated year (end of January), the adult population was reset to 200 super-adults. Population growth was then then number of adults after 12 months, the following January, divided by 200. The super-individual approach was developed to speed up computation time by avoiding very large numbers of simulated individuals while also avoiding 'crashes' when the simulated population declines to zero.

The model is initialized with adult spawners in February and assumed weights of adult delta smelt, generated from a lognormal distribution. Weights are converted to lengths using the length-weight equation derived by Kimmerer et al. (2005),

$$L_{\mathrm{iym}} = \sqrt[3.82]{\frac{W_{\mathrm{iym}}}{1.83e^{-6}}}, \quad \text{(A1)}$$

where W_{iym} is weight in grams and L_{iym} is fork length in millimeters of individual i in year y and month m of the simulation.

Reproduction. Four reproductive sub-processes are modeled: maturation, sex ratio, fecundity, and egg to larval survival. Simulated delta smelt reproduction occurs during the months of February, March, and April. During spawning months, maturity is stochastically assigned using a Bernoulli distribution and a length-based, logistic regression model of maturation probability

$$mature_{\mathrm{iym}} \sim \mathrm{Bernoulli}\left(1/\left(1+e^{-0.1*(L_{\mathrm{iym}}-60)}\right)\right), \quad \text{(A2)}$$

where 60 mm represented an assumed length at 50% maturity and 0.1 represents an assumed slope coefficient. With this maturation model, the probability of maturity increases from approximately 0.05 at 48 mm to 0.95 at 72 mm (Fig. A4). This is in contrast to the IBM, which used a knife-edged

maturation model, in which individuals less than 60mm FL had no probability of maturation and spawning.

Sex is also stochastically assigned to simulated fish using a Bernoulli distribution, with a 0.48 probability of female assignment, based on Spring Kodiak Trawl samples of adult delta smelt during the spawning season

(A3) $female_{\mathrm{i}} \sim \mathrm{Bernoulli}(0.48)$.

Water temperature is assumed to affect several components of the reproductive and early life history of delta smelt, including the number of potential batch spawns, egg to larval survival, and length at first feeding (Rose et al. 2013a). Mature females spawn up to three batches of eggs, with one potential batch in both February and March and an April batch if an individual occupies a stratum with *Temp* < 17.9°C, based on the maximum observed spawning temperatures noted by Damon et al. (2016). Population egg production is based on the distribution of L, the length-based fecundity model estimated by Damon et al. (2016) (Fig. A4), and the simulated abundance of mature females (adults; AD) in each year-month-stratum $n_{\mathrm{AD_{yms}}}|female, mature$. Total egg production in each year-month-stratum $n_{\mathrm{Egg_{yms}}}$ of the spawning season is the sum of fecundity of mature females in that stratum

(A4) $n_{\mathrm{Egg_{yms}}} = \sum_{j=1}^{n_{\mathrm{AD_{yms}}}|female,mature} 0.0183 * L_{\mathrm{jym}}^{2.7123}$.

Simulated eggs transition to feeding larvae at the end of the month of spawning. Survival of eggs to the larval life stage $S_{\mathrm{LRV_{ym}}}$ (Fig. A5) is the product of proportion hatching $P_{\mathrm{Hatch_s}}$ and egg to larval survival $S_{\mathrm{YS_{yms}}}$,

(A5) $S_{\mathrm{LRV_{yms}}} = P_{\mathrm{Hatch_s}} * S_{\mathrm{YS_{yms}}}$, where

(A6) $P_{\mathrm{Hatch_s}} = -2.35 + 0.45 * Temp_{\mathrm{yms}} + 0.016 * Temp_{\mathrm{yms}}^2$ and

(A7) $S_{\mathrm{YS_{yms}}} = e^{-0.035*\left(-10.1-1.5*Temp_{\mathrm{yms}}\right)}$.

Parameters defining the $P_{\mathrm{Hatch_s}}$ and $S_{\mathrm{YS_{yms}}}$ models (Eq. A6-7) were given by Bennett (2005) (Bennett's Fig. 10) and included temperature effects. Number of days as a yolk-sac larvae $(-10.1 - 1.5 * Temp_{\mathrm{yms}})$ is multiplied by daily yolk-sac larval mortality of 0.035 (Eq. A7), estimated by Rose et al. (2013a), to predict $S_{\mathrm{YS_{yms}}}$.

Initial simulated lengths L_{LRV} for larvae at the end of their first month, before entering the feeding population in the bioenergetics model, are calculated

(A8) $L_{\mathrm{LRV_i}} = 5.92 - 0.05 * Temp_{\mathrm{yms}}$,

and $L_{\mathrm{LRV_i}}$ are converted to weights using the larval length-weight equation derived by Kimmerer et al. (2005),

(A9) $W_{\mathrm{iym}} = 5e^{-6} * L_{\mathrm{iym}}^3$.

Movement. A Eulerian random walk model was developed to simulate delta smelt movement among spatial strata that approximates the observed spatial distributions of the population. Fish are randomly assigned to one of n_{STR} spatial strata based on observed spatial distributions DS_{yms} and a set of rules for movement. Starting strata for each individual *i* at the end of January 1995 are categorically distributed, with probabilities equal to DS_{yms}

(A10) $strata_{\mathrm{iym}} \sim \mathrm{Categorical}\left(DS_{\mathrm{yms}}\right)$.

Starting strata for newly spawned fish are assigned to the parental spatial strata. In each subsequent month, categorical distribution probabilities to randomly assign strata are the product of observed spatial distributions and a set of rules for month-to-month movement that allow residence in a stratum, movement between adjacent strata, or movement between strata separated by only a single stratum. The movement rules prevent simulated movement to more distant strata (e.g., month-to-month movement between Yolo and Suisun Bay strata is not modeled). Rules for movement between stratum s and s′ are represented by an n_{STR} x n_{STR} matrix $R_{\mathrm{ss}\prime}$ of 1s and 0s, where 1s permit simulated movement between a pair of spatial strata and 0s prevent simulated movement

(A11) $strata_{\mathrm{iym}} \sim \mathrm{Categorical}\left(DS_{\mathrm{yms}} * R_{\mathrm{s}(1:n_{\mathrm{STR}})}\right)$.

Growth. The bioenergetics growth model described by Rose et al. (2013a) was a version of the 'Wisconsin model', a system of equations estimating daily growth in body mass as a function of rates of consumption C_{iym}, metabolism R_{iym}, egestion F_{iym}, excretion U_{iym}, activity SDA_{iym} and spawning losses Sp_{iym} for individual *i* in year *y* and month *m* (Eqs. 12-24). In this application, daily growth increments were scaled to monthly increments by multiplying by the number of days in each month. A set of bioenergetics model coefficients, specific to each life-stage *l* to model each rate were listed in Rose et al. (2013a) (Fig. A7). These coefficients were borrowed from another smelt species, the Rainbow smelt *Osmerus mordax* (Lantry and Stewart 1993), with adjustments to temperature effects on consumption and maximum potential consumption. In the notation below, these fixed coefficients are denoted with a hat (^) to distinguish them from dynamic quantities that may vary by time period.

(A12) $W_{\mathrm{iy(m+1)}} = W_{\mathrm{iym}} * n.days_m * \frac{ep_{\mathrm{iym}}}{4814} * \left(C_{\mathrm{iym}} - R_{\mathrm{iym}} - F_{\mathrm{iym}} - U_{\mathrm{iym}} - SDA_{\mathrm{iym}}\right) - Sp_{\mathrm{iym}}$, where

(A13) $R_{\mathrm{iym}} = \widehat{ar}_{\mathrm{l}} * W_{\mathrm{iym}}^{\widehat{br}_{\mathrm{l}}} * e^{\widehat{RQ}_{\mathrm{l}} * Temp_{\mathrm{yms}}}$,

(A14) $F_{\mathrm{iym}} = \widehat{Fa}_{\mathrm{l}} * C_{\mathrm{iym}}$,

(A15) $U_{\mathrm{iym}} = \widehat{Ua}_{\mathrm{l}} * \left(C_{\mathrm{iym}} - F_{\mathrm{iym}}\right)$,

(A16) $SDA_{\mathrm{iym}} = \widehat{Sa}_{\mathrm{l}} * \left(C_{\mathrm{iym}} - F_{\mathrm{iym}}\right)$, and

(A17) $Sp_{\mathrm{iym}} = 0.15 * W_{\mathrm{iym}}$

The conversion of prey to delta smelt biomass was expected to be less efficient for *Limnoithona* prey because of its lower energy density ed_{p}. The lower ed_{p} of *Limnoithona* was accounted by

adjusting the efficiency at which simulated consumption was converted to delta smelt weight, represented by the ratio $ep_{iym}/4814$ (Eq. A12). ep_{iym} was the energy density of prey consumed, reduced by the fraction of consumed energy corresponding to *Limnoithona* (Eq. A18 and A19), and 4,814 J/g was the energy density of delta smelt. The energy density of *Limnoithona* (1,813 J/g) was assumed to be 30% less than that of all other prey items (2,590 J/g).

(A18) $ep_{\mathrm{iym}} = 1813 * Limno_{\mathrm{iym}} + 2590 * \left(1 - Limno_{\mathrm{iym}}\right)$, where

(A19) $$Limno_{\mathrm{iym}} = \frac{1813 * Cmax_{\mathrm{iym}} * \left(\frac{\frac{PD_{\mathrm{ym(LImno)}} * \hat{V}_{\mathrm{(Limno)l}}}{\hat{K}_{\mathrm{(Limno)l}}}}{\sum_{r=1}^{12} \frac{PD_{\mathrm{ymr}} * \hat{V}_{\mathrm{rl}}}{\hat{K}_{\mathrm{rl}}}} \right)}{\sum_{q=1}^{12} \widehat{ed}_{\mathrm{q}} * Cmax_{\mathrm{iym}} * \left(\frac{\frac{PD_{\mathrm{ymq}} * \hat{V}_{\mathrm{ql}}}{\hat{K}_{\mathrm{ql}}}}{\sum_{r=1}^{12} \frac{PD_{\mathrm{ymr}} * \hat{V}_{\mathrm{rl}}}{\hat{K}_{\mathrm{rl}}}} \right)}$$ and

where PD_{ymp} was the prey density of prey type p.

The maximum possible consumption rate $C_{\mathrm{max_{iym}}}$ was a measure of potential foraging rate, expressed as a proportion of body weight per day (Eqs. A20 and A21). Foraging arena theory suggests that fish reduce their time spent foraging to mitigate perceived risk of mortality, at the expense of forgone foraging and growth. Two environmental constraints on delta smelt foraging were considered: temperature $Temp_{\mathrm{ym}}$ effects ($KA_{\mathrm{iym}} * KB_{\mathrm{iym}}$) and turbidity $Turb_{\mathrm{iym}}$ effects (KT_{iym}). Relationships between *Temp*, *C*, and *R* are shown in Fig. A6.

(A20) $$C_{\mathrm{iym}} = C_{\mathrm{max_{iym}}} * \sum_{q=1}^{12} \left(\frac{\frac{PD_{\mathrm{ymp}} * \hat{V}_{\mathrm{ql}}}{\hat{K}_{\mathrm{ql}}}}{\sum_{r=1}^{12} \frac{PD_{\mathrm{ymp}} * \hat{V}_{\mathrm{rl}}}{\hat{K}_{\mathrm{rl}}}} \right)$$, where

(A21) $$C_{\mathrm{max_{iym}}} = \widehat{ac}_{\mathrm{l}} * W_{\mathrm{iym}}^{\widehat{bc}_{\mathrm{l}}} * KA_{\mathrm{yms}} * KB_{\mathrm{yms}} * KT_{\mathrm{yms}}$$

Rose et al. (2013) assumed a *Temp*-C_{max} model for delta smelt (KA_{yms} and KB_{yms}; Eq. A12 and A13) that reduced foraging time as water temperatures increased above 23°C (Fig. A6).

(A22) $$KA_{\mathrm{yms}} = \frac{\widehat{CK1}_{\mathrm{l}} * e^{\frac{1}{\widehat{TO}_{\mathrm{l}} - \widehat{CQ}_{\mathrm{l}}} * ln\left(\frac{0.98 * \left(1 - \widehat{CK1}_{\mathrm{l}}\right)}{0.02 * \widehat{CK1}_{\mathrm{l}}}\right) * \left(Temp_{\mathrm{yms}} - \widehat{CQ}_{\mathrm{l}}\right)}}{1 + \widehat{CK1}_{\mathrm{l}} * \left(e^{\frac{1}{\widehat{TO}_{\mathrm{l}} - \widehat{CQ}_{\mathrm{l}}} * ln\left(\frac{0.98 * \left(1 - \widehat{CK1}_{\mathrm{l}}\right)}{0.02 * \widehat{CK1}_{\mathrm{l}}}\right) * \left(Temp_{\mathrm{yms}} - \widehat{CQ}_{\mathrm{l}}\right)} \right) - 1)}$$

(A23) $$KB_{\mathrm{yms}} = \frac{\widehat{CK4}_{\mathrm{l}} * e^{\frac{1}{\widehat{TL}_{\mathrm{l}} - \widehat{TM}_{\mathrm{l}}} * ln\left(\frac{0.98 * \left(1 - \widehat{CK4}_{\mathrm{l}}\right)}{0.02 * \widehat{CK4}_{\mathrm{l}}}\right) * \left(\widehat{TL}_{\mathrm{l}} - Temp_{\mathrm{yms}}\right)}}{1 + \widehat{CK4}_{\mathrm{l}} * \left(e^{\frac{1}{\widehat{TL}_{\mathrm{l}} - \widehat{TM}_{\mathrm{l}}} * ln\left(\frac{0.98 * \left(1 - \widehat{CK4}_{\mathrm{l}}\right)}{0.02 * \widehat{CK4}_{\mathrm{l}}}\right) * \left(\widehat{TL}_{\mathrm{l}} - Temp_{\mathrm{yms}}\right)} \right) - 1)}$$

Forage fish, such as delta smelt, typically show a decrease in foraging rates as turbidity declines and the perceived risk of being detected by a predator increases (Pangle et al. 2012). The risk of

predation and changes in delta smelt behavior in clear water were documented by Ferrari et al. (2014), though rates of predation may have been biased high because smelt could not effectively evade predators in laboratory conditions. The relationship between delta smelt foraging rate and turbidity reported by Hasenbein et al. (2016) was approximated using a simple logistic model (Fig. A2), that increased from the lowest turbidities evaluated (5 NTU; 84 cm Secchi depth) to the turbidities associated with maximum foraging rate (25-80 NTU; 28-13 cm Secchi depth). Since turbidities greater than 80 NTU were rarely observed during the time period explored, foraging limitation at high turbidity was not modeled, i.e., using a dome-shaped double-logistic model. As turbidity declined, the effect of turbidity (KT_{yms}; Eq. A14) was assumed to reach some asymptotic minimum $\hat{\alpha}_{FL}$.

(A24) $KT_{\mathrm{yms}} = \hat{\alpha}_{FL} + (1 - \hat{\alpha}_{FL})/\left(1 + e^{0.1*\left(Turb_{\mathrm{yms}} - 56.2\right)}\right)$

Mortality. The survival probability of simulated juvenile to adult delta smelt $S_{\mathrm{JA}_{\mathrm{iym}}}$ is the function of two competing sources of mortality, entrainment mortality *F* and natural mortality *M* (Fig. A8)

(A25) $S_{\mathrm{JA}_{\mathrm{iym}}} = e^{-\left(F_{\mathrm{iym}} + M_{\mathrm{iym}}\right)}$.

F represents the effect of being drawn into the South Delta through the action of pumping, where fish may be subject to direct export from the system, predation in the South Delta, or otherwise isolation from the remainder of the population. *M* represents all other sources of mortality. Natural mortality in IBMR predominantly represents predation, as the effects of food and starvation are accounted with bioenergetics.

The survival state of each individual z_{iym} (1 or 0) is randomly assigned to each individual based on draws from a Bernoulli distribution with probability $S_{\mathrm{JA}_{\mathrm{iym}}}$

(A26) $z_{\mathrm{iym}} \sim \mathrm{Bernoulli}\left(S_{\mathrm{JA}_{\mathrm{iym}}}\right)$.

Simulated fish may also die due to starvation, if their weight declines more than 15% during a one-month period.

F is applied to fish located in the South Delta stratum during December–June. A 'ramp' model of *F* as a function of *OMR* is used to calculate the level of *F* to apply (Fig. A8). If *OMR* is less than or equal to the minimum threshold (-5,000 ft^3/s for larger fish and -3,500 ft^3/s for smaller fish), all fish occupying the South Delta experience entrainment mortality; at the simulated population level, the entrainment loss equals that estimated by the US Fish and Wildlife Service's Life Cycle Model (Smith et al. 2021). *F* declines linearly to zero from the LCM-based level, as *OMR* increases to 0 ft^3/s. Fish located outside of the South Delta are assigned $F = 0$; all fish are assigned $F = 0$ during July–November.

Rose et al. (2013b) defined a length-based *M* model $M_{\mathrm{iym}} = -0.034 + 0.165 * L_{\mathrm{iym}}^{-0.322}$. The same length-based model of *M* is assumed in IBMR, but it is scaled in proportion to the *Secchi*-$C_{\max}$ relationship (KT_{iym}; Eq. A24). It is assumed that the length-based model represented a maximum potential rate of *M*, and that delta smelt experience lower predation risk as turbidity increases. As

turbidity increases and predation risk declines, delta smelt respond by increasing foraging rate (the *Secchi*-$C_{\max}$ relationship). In other words, this approach assumes that delta smelt limit foraging in proportion to the predation risk they perceive as turbidity varies. Although the experiments of Ferrari et al. (2014) demonstrated a mechanism relating lower turbidity to higher predation of delta smelt, these results may have been biased by the confined, artificial conditions of the experiment. Wild delta smelt are expected to experience less predation mortality compared to what Ferrari et al. (2014) documented in a lab setting. Under poor foraging conditions, represented by low turbidity, foraging is minimized ($KT_{\text{iym}} = \hat{\alpha}_{FL}$) and natural mortality is maximized at the rate predicted by the length-based *M* model. Under ideal conditions of higher turbidity, foraging is maximized ($KS_{\text{iym}} = 1$) and natural mortality is minimized at the $\hat{\alpha}$ fraction of delta smelt natural mortality predicted by the length-based *M* model.

(27) $$M_{\text{iym}} = \left(-0.034 + 0.165 * L_{\text{iym}}^{-0.322}\right) * \left(1 - \hat{\alpha}_{FL} + KT_{\text{iym}}\right).$$

Population growth. Annual growth of the simulated delta smelt population is defined by spawner abundance (AB), or the number of fish in the simulated population just prior to the beginning of the spawning season in February. Annual population growth $\lambda_{\text{AB}_\text{y}}$ is calculated

(28) $$\lambda_{\text{AB}_\text{y}} = \frac{AB_y}{AB_{y-1}}.$$

Model calibration and diagnostics. M and the maximum turbidity penalty on foraging $\hat{\alpha}$ were calibrated so that the simulated delta smelt population reproduced certain qualities of the wild delta smelt population. *M* required calibration to generate the long-term patterns in delta smelt abundance observed across fish surveys. $\lambda_{\text{AB}_\text{y}}$ were the product of reproductive, survival, and individual growth rates. IBMR survival rates (i.e., *M*) were calibrated to approximate the population growth rates estimated in the wild population (Smith et al. 2021; Fig. A9). The geometric mean of observed population growth rates, calculated from 1995-2014 June abundance estimates was 0.9. To calibrate IBMR to observed abundances, M_{iym} were iteratively multiplied by a constant until the median geometric mean λ_{AB} among IBMR-simulated June abundance time series was approximately 0.9. June abundances were used in this calibration, in order to leverage one of the better observed delta smelt abundance datasets using the 20mm Survey.

The growth of simulated delta smelt depended on biotic and abiotic constraints on foraging. Biotic constraints were described by prey type and availability and the multispecies functional response (Eq. A20). Abiotic constraints were described by temperature and turbidity effects on $C_{\max}$ (Eq. A22-A24), which are only partially informed by experimental results; thus, temperature and turbidity effects on $C_{\max}$ represent a critical uncertainty in IBMR dynamics. In order to assess whether IBMR reproduced the expected growth trajectory for delta smelt, simulated mean length at age was compared to two reference points: a von Bertalanffy growth model fit to lengths and ages observed in the wild population (Smith and Nobriga 2023; Fig. A10) and mean lengths of delta smelt observed in February fish surveys (Fig. A11). The maximum effect of low turbidity on consumption rates $\hat{\alpha}$ was calibrated to observed February lengths by iteratively changing $\hat{\alpha}$ to minimize the residual (observed lengths – IBMR-predicted lengths) sum of squares for years 2002-2014, when the initiation of Spring Kodiak Trawl sampling reduced the length-selectivity bias of

the observed mean February lengths. Prior to 2002, mean observed lengths may have been biased low by the selectivity of the Midwater Trawl gear, which appears to decline for larger delta smelt (Mitchell et al. 2019).

References

Bennett, W. A. 2005. Critical assessment of the delta smelt population in the San Francisco Estuary, California. San Francisco Estuary and Watershed Science 3(2).

Damon, L. J., S. B. Slater, R. D. Baxter, and R. W. Fujimura. 2016. Fecundity and reproductive potential of wild female Delta Smelt in the upper San Francisco Estuary, California. California Fish Game 102: 188–210.

Ferrari, M. C., L. Ranåker, K. L. Weinersmith, M. J. Young, A. Sih, and J. L. Conrad. 2014. Effects of turbidity and an invasive waterweed on predation by introduced largemouth bass. Environmental biology of fishes 97(1): 79–90.

Hasenbein, M., N. A. Fangue, J. Geist, L. M. Komoroske, J. Truong, R. McPherson, and R. E. Connon. 2016. Assessments at multiple levels of biological organization allow for an integrative determination of physiological tolerances to turbidity in an endangered fish species. Conservation physiology 4(1): 1–16.

Kimmerer, W., S. R. Avent, S. M. Bollens, F. Feyrer, L. F. Grimaldo, P. B. Moyle, M. Nobriga, and T. Visintainer. 2005. Variability in length–weight relationships used to estimate biomass of estuarine fish from survey data. Transactions of the American Fisheries Society 134: 481–495.

Kurobe, T., M. O. Park, A. Javidmehr, F. C. Teh, S. C. Acuña, C. J. Corbin, A. J. Conley, W. A. Bennett, and S. J. Teh. 2016. Assessing oocyte development and maturation in the threatened Delta Smelt, Hypomesus transpacificus. Environmental biology of fishes 99(4): 423–432.

LaCava, M., K. Fisch, M. Nagel, J. C. Lindberg, B. May, and A. J. Finger. 2015. Spawning behavior of cultured Delta Smelt in a conservation hatchery. North American Journal of Aquaculture 77(3): 255–266.

Lantry, B. F., and D. J. Stewart. 1993. Ecological energetics of Rainbow Smelt in the Laurentian Great Lakes: an interlake comparison. Transactions of the American Fisheries Society 122:951–976.

Pangle, K. L., T. D. Malinich, D. B. Bunnell, D. R. DeVries, and S. A. Ludsin. 2012. Context-dependent planktivory: interacting effects of turbidity and predation risk on adaptive foraging. Ecosphere 3(12):114.

Peterson, J., E. McCreless, A. Duarte, S. Hamilton, and J. Medellin-Azuara. 2019. Structured Decision Making for Scientific Management in the San Francisco Bay-Delta. Draft progress report, US Bureau of Reclamation, Sacramento, CA.

R Core Team. 2022. R version 4.2.2: A language and environment for statistical computing. R Foundation for Statistical Computing, Vienna, Austria. URL http://www.R-project.org/.

Rose, K. A., W. J. Kimmerer, K. P. Edwards, and W. A. Bennett. 2013a. Individual-based modeling of delta smelt population dynamics in the upper San Francisco Estuary: I. Model description and baseline results. Transactions of the American Fisheries Society 142: 1238–1259.

Rose, K. A., W. J. Kimmerer, K. P. Edwards, and W. A. Bennett. 2013b. Individual-based modeling of Delta Smelt population dynamics in the upper San Francisco Estuary: II. Alternative baselines and good versus bad years. Transactions of the American Fisheries Society 142: 1260–1272.

Smith, W. E. 2018. Delta Smelt Model Technical Note 35: Delta smelt growth model. US Fish and Wildlife Service, Bay-Delta Office, Sacramento, CA. Technical Report.

Smith, W. E, L. Polansky, and M. L. Nobriga. 2021. Disentangling risks to an endangered fish: using a state-space life cycle model to separate natural mortality from anthropogenic losses. Canadian Journal of Fisheries and Aquatic Sciences. *In press*. doi: 10.1139/cjfas-2020-0251.

Table A1. Version history of delta smelt individual-based models, with the date of version development increasing from left to right. Modifications to the model, from the previous version, are indicated in bold.

Model component	Model version			
	IBMv1	IBMv2	IBMRv1	IBMRv2
Time series	1995-2005	**1991-2011**	1995-**2014**	1995-2014
Spatial strata	11 strata: Upper Sacramento, East Delta, South Delta, Lower San Joaquin, Lower Sacramento, Confluence, Southeast Suisun, Northeast Suisun, Suisun Marsh, Southwest Suisun, Northwest Suisun	**12 strata: Yolo Bypass and Cache Slough**, Upper Sacramento, East Delta, South Delta, Lower San Joaquin, Lower Sacramento, Confluence, Southeast Suisun, Northeast Suisun, Suisun Marsh, Southwest Suisun, Northwest Suisun	12 strata	12 strata
Time step	Daily	Daily	**Monthly**	**Bioenergetics: daily**; Movement, survival, spawning: monthly
Movement	Particle tracking model for larvae, salinity-based behaviors for later life stages	Particle tracking model for larvae, salinity-based behaviors for later life stages	**Based on observed distribution in surveys**	Based on observed distribution in surveys
Prey selection	Holling type-2 functional response	Holling type-2 functional response	Holling type-2 functional response	Holling type-2 functional response
Number of prey types	6	**12 (Slater et al. 2014)**	12	12

Table A1 continued.

Model component	Model version			
	IBMv1	IBMv2	IBMRv1	IBMRv2
Spawning	Bennett (2005) fecundity model; number of batches based on refractory period; thermal limit = 20C; 2-year life cycle	**Damon et al. (2016) fecundity model and thermal limit (17.9C); no more than 3 batches (LaCava et al. 2015; Kurobe et al. 2016); 1-year life cycle**	Damon et al. fecundity model and thermal limit; no more than 3 batches	Damon et al. (2016) fecundity model and thermal limit (17.9C); no more than 3 batches
Egg hatch rate	Bennett (2005) hatching success model	Bennett (2005) hatching success model	Bennett (2005) hatching success model	Bennett (2005) hatching success model
Egg survival	Bennett (2005) temperature dependent model	Bennett (2005) temperature dependent model	Bennett (2005) temperature dependent model	Bennett (2005) temperature dependent model
Length at hatch	Bennett (2005) temperature dependent model	Bennett (2005) temperature dependent model	Bennett (2005) temperature dependent model	Bennett (2005) temperature dependent model
Larval development rate	Bennett (2005) temperature dependent model	Bennett (2005) temperature dependent model	Bennett (2005) temperature dependent model	Bennett (2005) temperature dependent model
Larval survival	$e^{-0.035}/d$ay	**Recalibrated**	$e^{-0.035}/day$	$e^{-0.035}/day$
Entrainment	Based on 1-D hydrodynamics and other fitting	Based on 1-D hydrodynamics and other fitting	**Based on estimates of proportional entrainment (Smith et al. 2021)**	Based on estimates of proportional entrainment

Table A1 continued.

Model component	Model version			
	IBMv1	IBMv2	IBMRv1	IBMRv2
Bioenergetics	Rainbow smelt (Lantry and Stewart 1993), with adjustments to temperature sensitivity >23C	Rainbow smelt (Lantry and Stewart 1993), with adjustments to temperature sensitivity >23C	Rainbow smelt, with temperature sensitivity >23C; **turbidity limitation on consumption (Hasenbein et al. 2016)**	Rainbow smelt, **with temperature sensitivity >21.6C and daylength limitation on consumption (Smith and Nobriga 2023)**; turbidity limitation on consumption
Mortality	User-defined: Length-based or stage-based	User-defined: Length-based or stage-based	Length-based, **with turbidity effect**	Length-based, with turbidity effect
Super-individuals	Reset daily	Reset daily	**Reset annually**	Reset annually

Table A2. All indices, data, and simulated parameters used to denote IBMR.

Index	Description	Values
y	year	y = 1995, 1996, …2014
m	month	m = 2, 3, …12, 1
s	spatial strata	s = 1, 2, …12
p	prey type	p = 1, 2, …12
i	individual	i = 1, 2, …
Data	**Description**	
PD_{ymsp}	prey density	
OMR_{ym}	Old and Middle River flow	
DS_{yms}	observed delta smelt spatial distribution	
$Temp_{\mathrm{yms}}$	water temperature	
$Secchi_{\mathrm{yms}}$	Secchi depth	
$R_{ss'}$	matrix of movement rules between strata *s* and *s'*	
Simulated variables	**Description**	
L_{iym}	fork length	
W_{iym}	weight	
$mature_{\mathrm{iym}}$	maturity status	
$female_{\mathrm{i}}$	sex	
$n_{\mathrm{AD_{yms}}}$	abundance of adults	
$n_{\mathrm{Egg_{yms}}}$	number of eggs produced	
$S_{\mathrm{LRV_{ym}}}$	survival of eggs to the larval life stage	
$P_{\mathrm{Hatch_s}}$	probability of egg hatching	
$S_{\mathrm{YS_{yms}}}$	survival of yolk-sac larvae	
$L_{\mathrm{LRV_i}}$	larval length at first feeding	
$strata_{\mathrm{iym}}$	stratum occupied by individual *i*	
C_{iym}	realized consumption rate	
R_{iym}	respiration	
F_{iym}	egestion	
U_{iym}	excretion	
SDA_{iym}	activity	
Sp_{iym}	spawning loss	
C_{max}	maximum potential consumption	
$S_{\mathrm{JA_{iym}}}$	survival of juveniles through adults	
F_{iym}	instantaneous rate of entrainment mortality	
M_{iym}	instantaneous rate of natural mortality	
z_{iym}	survival status	
F_{max}	maximum potential rate of entrainment mortality	
z_{iym}	survival status	
D_{yms}	number of simulated fish per m^3 (density)	
$\lambda_{\mathrm{AB_y}}$	population growth rate	

Table A3. Prey types and corresponding taxonomic groups forming the simulated prey field available for Delta Smelt foraging.

Taxonomic group	Description
acartela	*Acartiella sinensis* (copepod) adults
eurytem	*Eurytemora affinis* (copepod) adults
pdiapfor	*Pseudodiaptomus forbesi* (copepod) adults
othcalad	Other calanoid copepod adults
pdiapjuv	*Pseudodiaptomus forbesi* copepodites
othcaljuv	Other calanoid copepodites
limno	*Limnoithona* spp. copepods (all stages)
othcyc	Other cyclopoid copepods (all stages)
allcopnaup	Copepod nauplii (all spp.)
daphnia	*Daphnia* spp. (cladocerans)
othclad	Other cladocerans
other	All other taxa

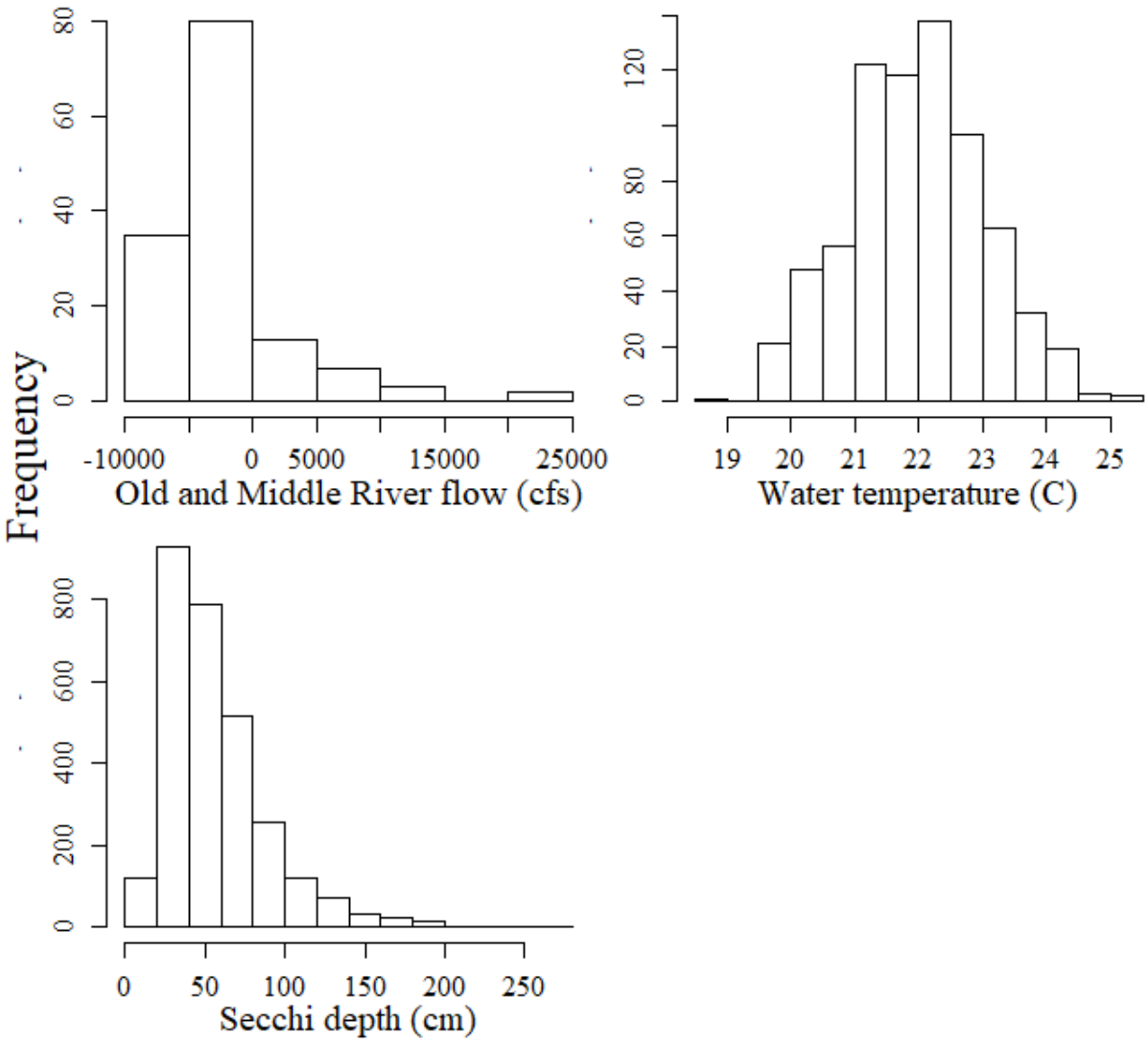

Figure A1. Histograms of physical Delta variables driving the Delta Smelt Individual-Based Life Cycls Model in R (IBMR). Old and Middle River flows for the critical December through June period and water temperatures for July through September are shown, because these variables were expected to be seasonally limiting. Secchi depths for all year-month-stratum combinations are shown.

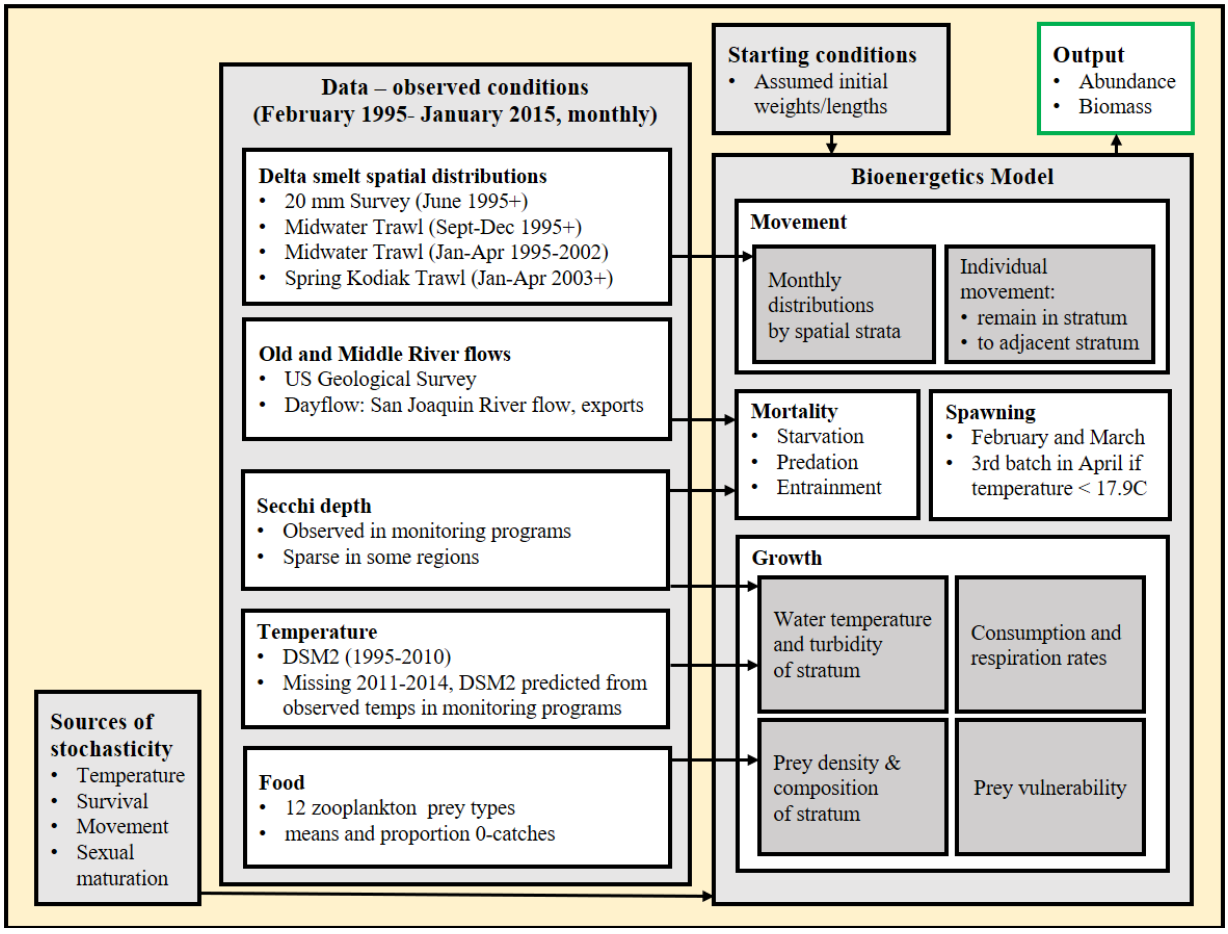

Figure A2. Diagram of the Delta Smelt Individual-Based Life Cycle Model in R (IBMR) and data.

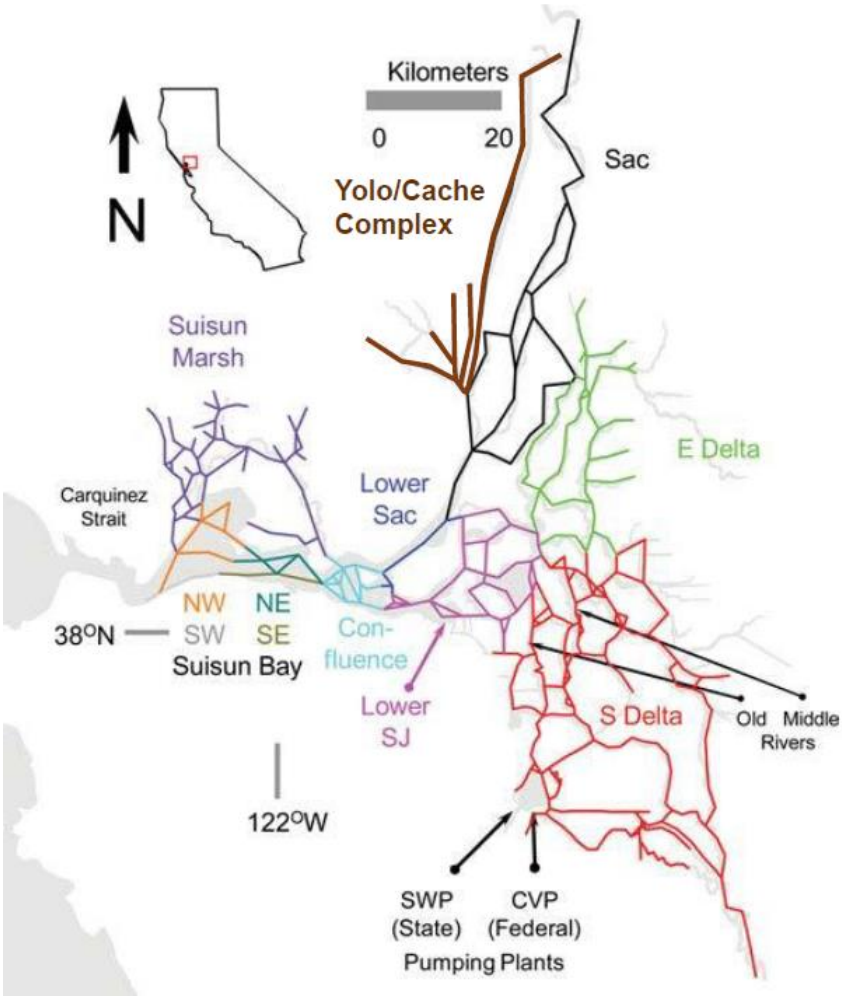

Figure A3. Map of the Sacramento-San Joaquin Delta, showing the spatial strata used to model delta smelt spatial distributions. This map was reproduced from Rose et al. (2013a) and Peterson et al. (2019).

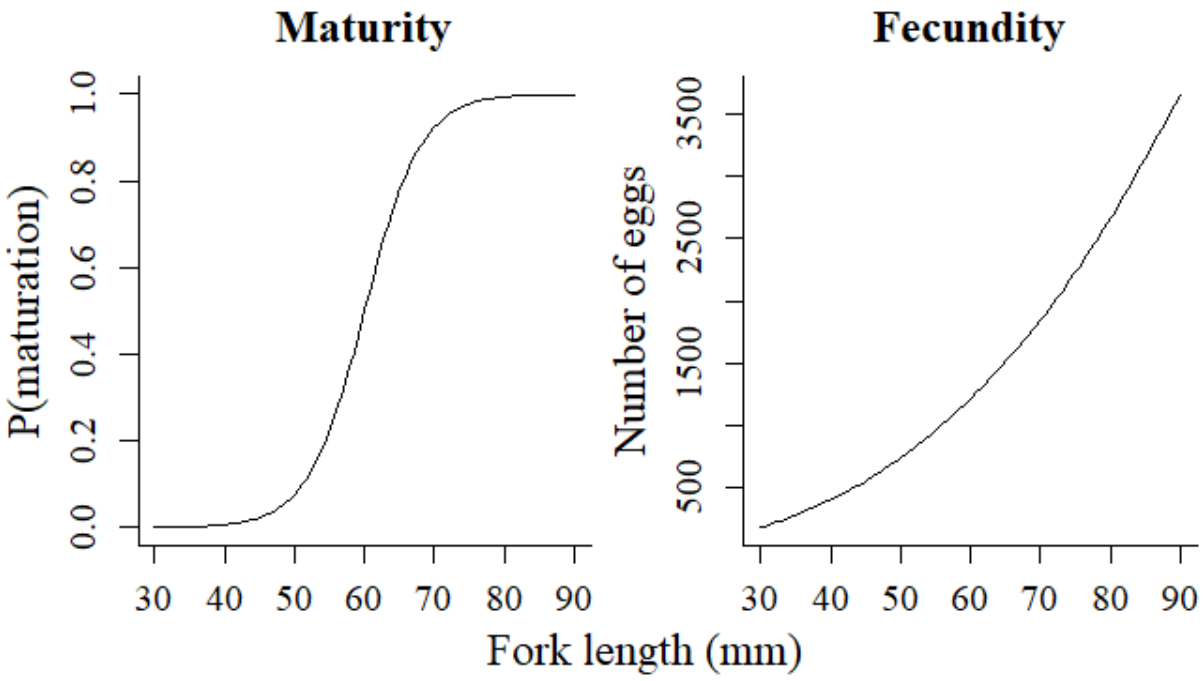

Figure A4. Models of the probability of maturation and fecundity at length.

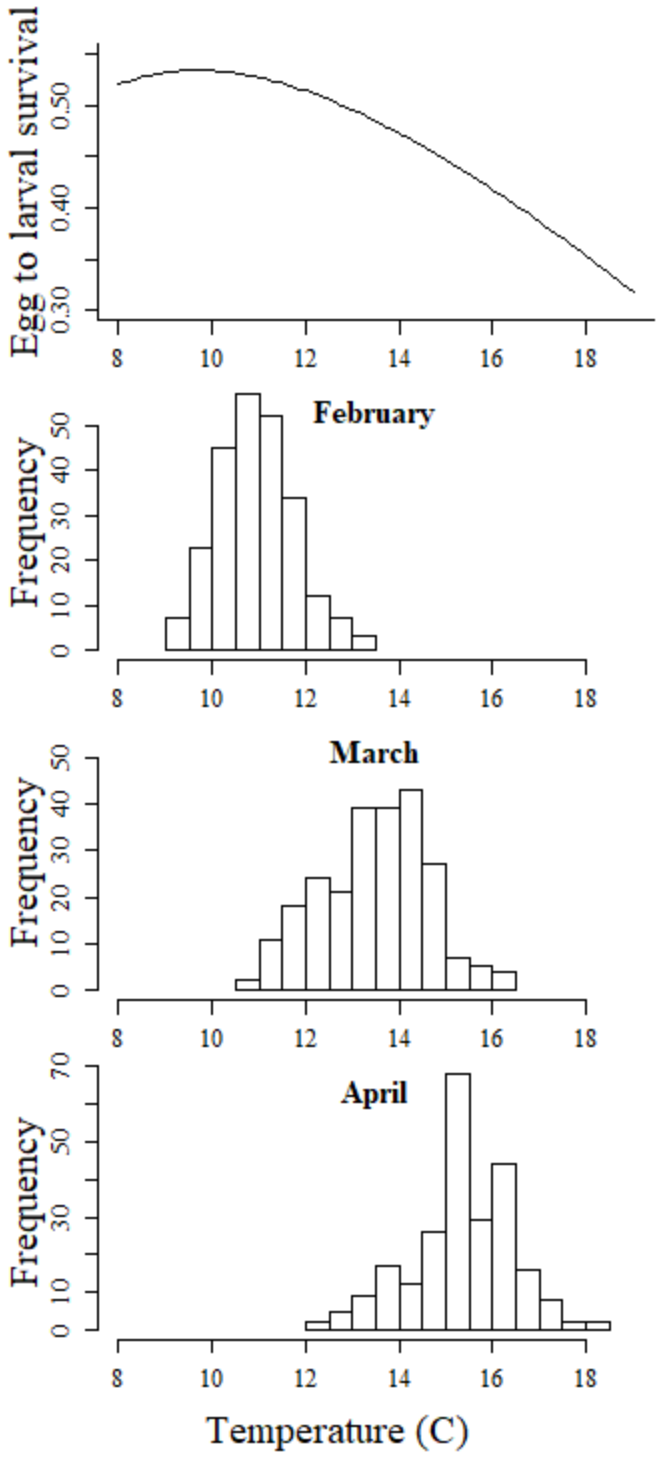

Figure A5. Model of egg to larval survival as a function of water temperature (top panel), based on Bennett (2005) (Bennett's Fig. 10). The bottom three panels show observed Delta temperatures in all spatial strata during spawning months of 1995-2014.

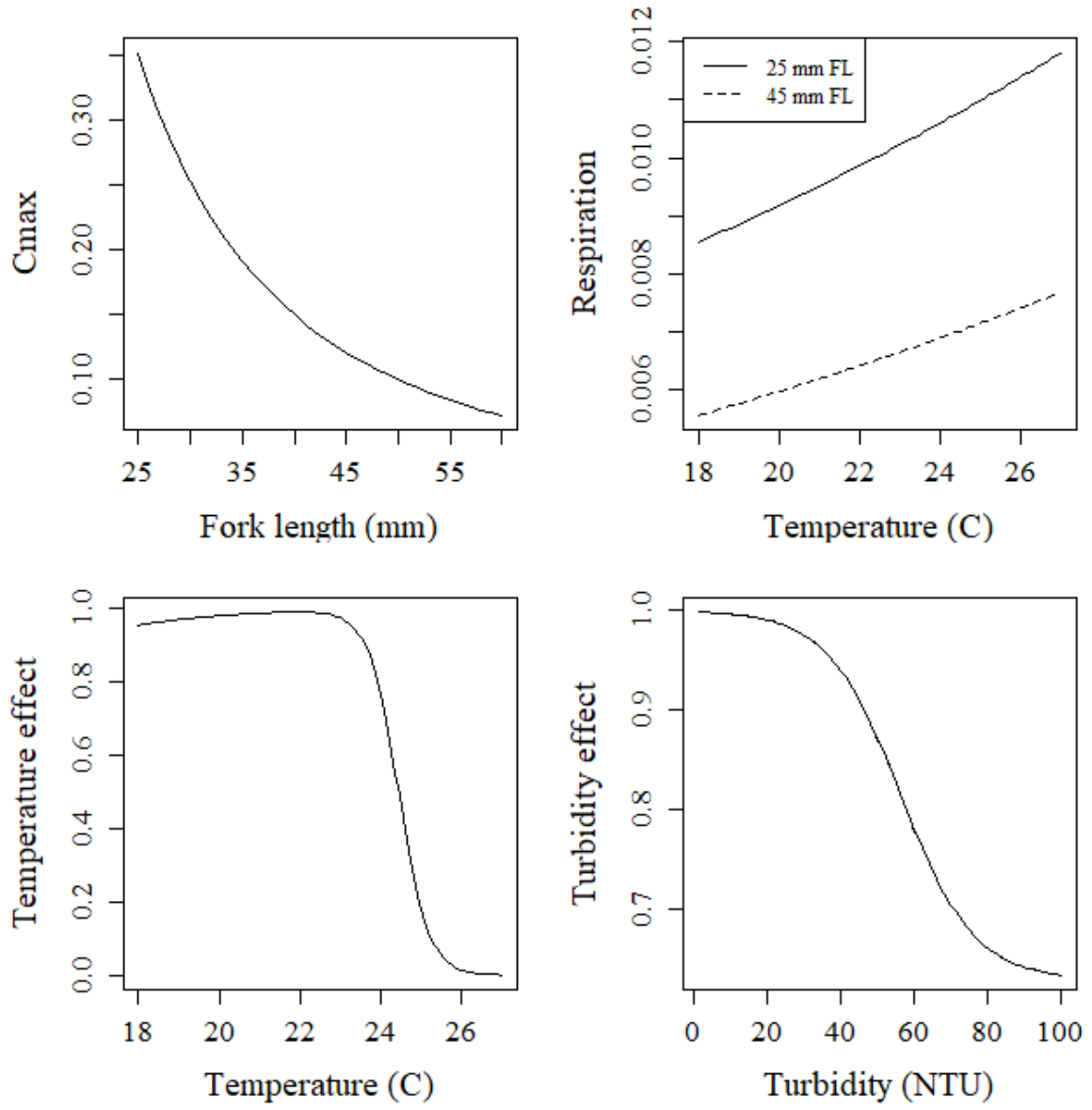

Figure A6. Models of maximum consumption (C_{max}) and respiration assumed by Rose et al. (2013a) (top row). In the bottom row are shown models of the temperature effect on C_{max} ($\boldsymbol{KA}_{\mathbf{iym}}$ and $\boldsymbol{KB}_{\mathbf{iym}}$; Eq. A12-13), and the model of the effect of turbidity on C_{max} ($\boldsymbol{KS}_{\mathbf{iym}}$; Eq. A14), suggested by data published by Hasenbein et al (2016).

TABLE 1. Parameter values for each Delta Smelt life stage in the bioenergetics model.

Parameter	Description	Larvae	Postlarvae	Juveniles and adults
	Maximum consumption (C_{max})			
a_c	Weight multiplier	0.18	0.18	0.1
b_c	Weight exponent	−0.275	−0.275	−0.54
CQ (°C)	Temperature at CK_1 of maximum	7	10	10
T_O (°C)	Temperature at 0.98 of maximum	17	20	20
T_M (°C)	Temperature at 0.98 of maximum	20	23	23
T_L (°C)	Temperature at CK_4 of maximum	28	27	27
CK_1	Effect at temperature CQ	0.4	0.4	0.4
CK_4	Effect at temperature T_L	0.01	0.01	0.01
	Metabolism (R)			
a_r	Weight multiplier	0.0027	0.0027	0.0027
b_r	Weight exponent	−0.216	−0.216	−0.216
R_Q	Exponent for temperature effect	0.036	0.036	0.036
S_d	Fraction of assimilated food lost to SDA	0.175	0.175	0.175
	Egestion (F) and excretion (U)			
F_a	Fraction of consumed food lost to egestion	0.16	0.16	0.16
U_a	Fraction of assimilated food lost to excretion	0.1	0.1	0.1

Figure A7. Table from Rose et al. (2013a) showing fixed parameter values used to simulate Delta Smelt feeding and growth.

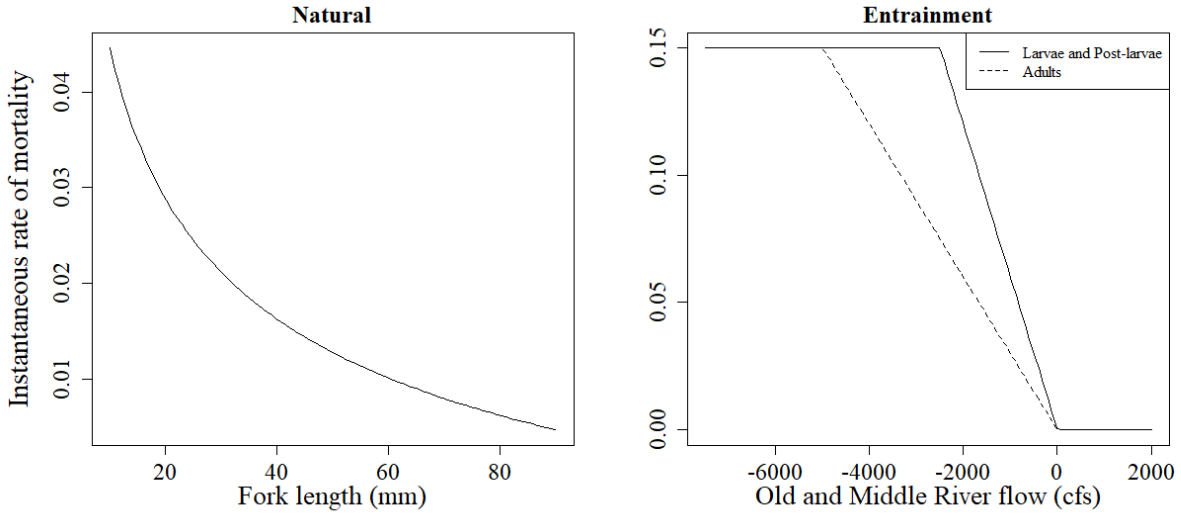

Figure A8. Models of instantaneous rates of natural (~ predation) and entrainment mortality. Entrainment mortality risk was added to natural mortality risk if fish occupied the South Delta stratum.

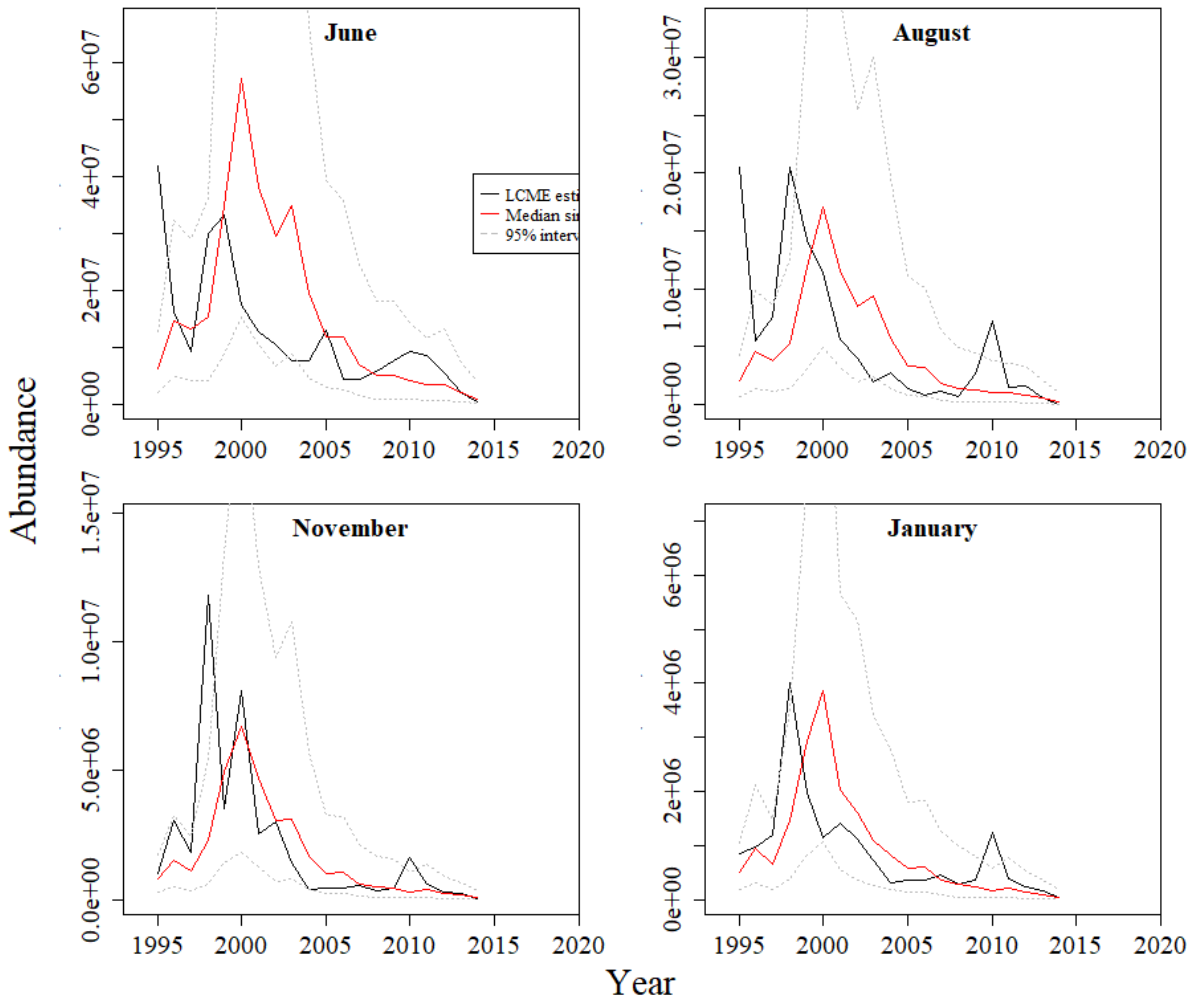

Figure 9. Median simulated abundance (red lines), among two simulated population time series (gray lines), and abundances estimated the Delta Smelt Life cycle Model with Entrainment (black lines) (Smith et al. 2021).

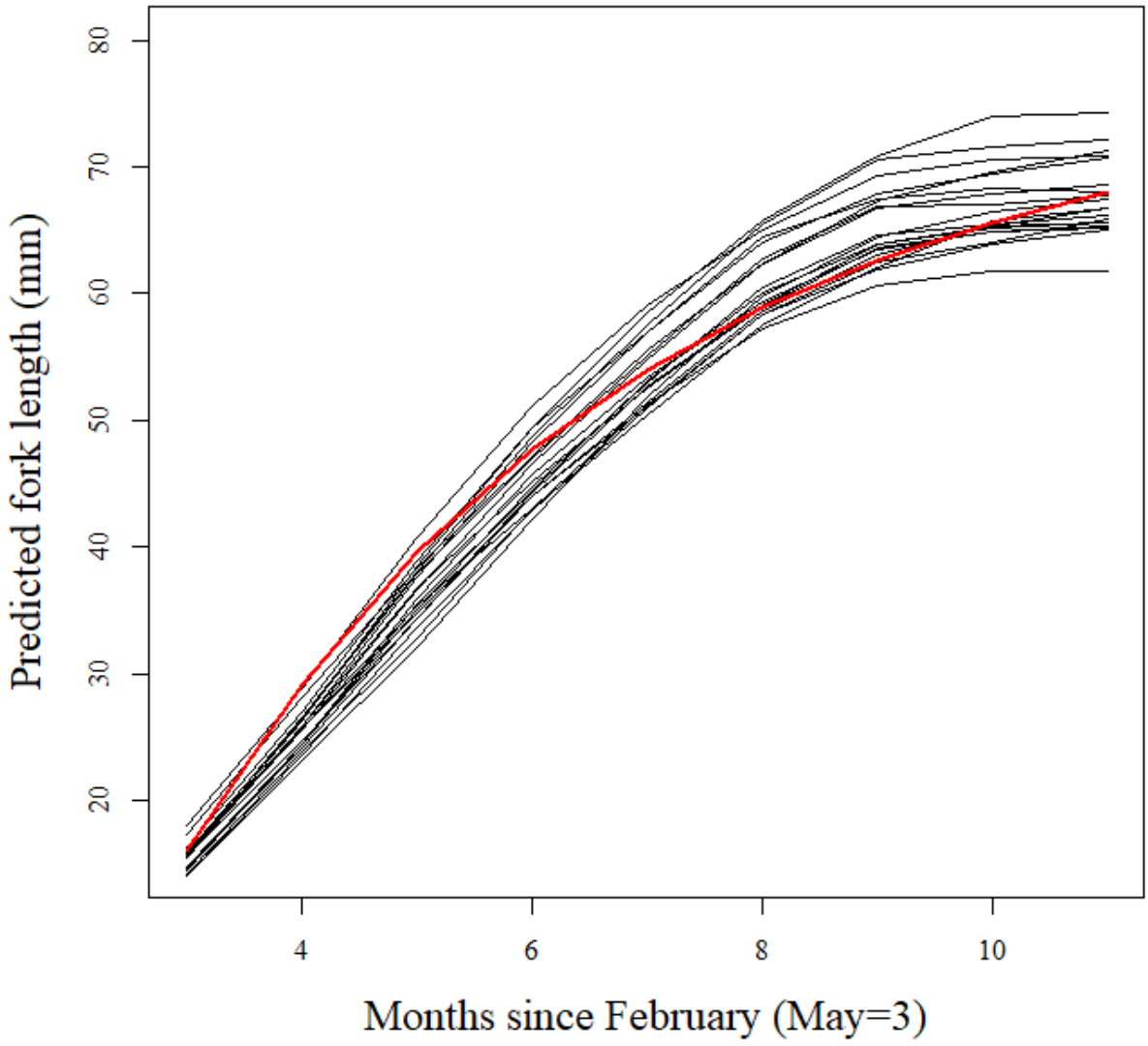

Figure A10. Simulated monthly time series of mean delta smelt length at age, for all years 1995-2015 (black lines) and von Bertalanffy growth model predicted length at age (red line), assuming a mean length of 16 mm FL in May. The von Bertalanffy model was fit to lengths and ages observed in the wild population.

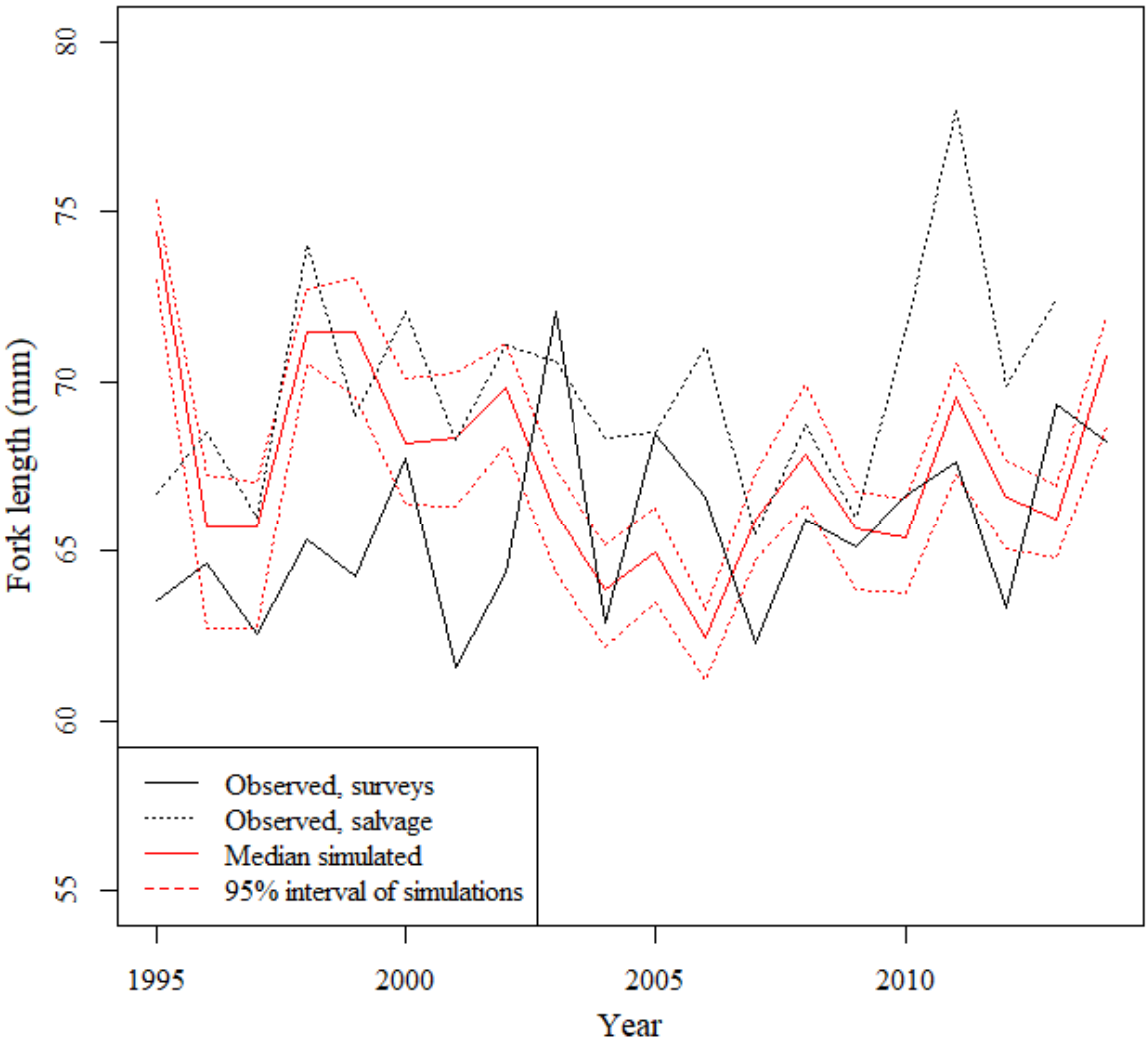

Figure A11. February fork lengths simulated by IBMR and observed for wild delta smelt in the CDFW Spring Kodiak (2002-2014), Midwater (1995-2001) Trawl Surveys, and in salvage operations.